SHIP REPORT 121

August 1968

NATIONAL PHYSICAL LABORATORY

SHIP DIVISION

WAVE PATTERNS ON THE SURFACE OF HYDRODYNAMIC CAVITIES

by

C. Brennen

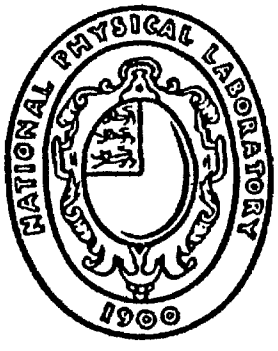

A Station of the
Ministry of Technology

Approved on behalf of Director, NPL by
Mr. J.A. Paffett, Superintendent of Ship Division

WAVE PATTERNS ON THE SURFACE OF HYDRODYNAMIC CAVITIES

by

C. Brennen

Ship Hydrodynamics Laboratory, N.P.L

SUMMARY

In experiments on cavities behind various axisymmetric headforms, a pattern of waves or ripples with crests parallel to the separation line was observed on the cavity surface just downstream of separation. A theoretical analysis suggests that this pattern results from amplified instabilities in the separated laminar boundary layer on the cavity surface.

1. INTRODUCTION

This paper reports an investigation into the stability and transition of the boundary layer flow on the surface of hydrodynamic cavities. The latter part is devoted to a study of the wave patterns observed on the interface in the neighbourhood of transition. However this theoretical investigation grew out of a wider qualitative study of the surface appearance of cavities, discussion of which makes up sections 2 and 3.

The experiments which were carried out in the No. 2 water tunnel of Ship Division, N.P.L. employed various rotationally symmetric shapes of headform supported on the axis of the tunnel by a sting and strut system described in earlier papers (Brennen (1968a and 1968b)). Despite this limitation to axisymmetric flows, some of the findings are expected to be qualitatively applicable to more general types of cavity flow.

In order to "freeze" the action in such flows it is necessary to photograph with an exposure of the order of microseconds; the equipment employed in the present investigation gave a flash of some 10→30μsecs. The experimental arrangement included provision for ventilating the cavities with measured flow rates of air and for measuring the cavity pressure as described in the earlier papers cited above. The normal tunnel equipment was used for measurement of tunnel pressure, velocity (0→45ft/sec) and temperature. The cavitation number and other data relevant to each photograph could thus be computed. Five different headforms were employed:

(a) a 3 in diameter sphere (plates 2 and 3)

(b) a 3 in diameter sphere cut off along a plane through the latitudinal line 68 degrees from the theoretical front stagnation point (referred to as the "cut-away" sphere) (plates 5 and 6).

(c) a $1_{1/8}$ in diameter hemispherical head placed on the end of the sting which was of the same diameter (plate 7).

(d) an ogival shaped head of axial length $3\frac{1}{2}$ in and base diameter 2.34 in (plates 1 and 4), whose shape corresponded to that of a theoretical semi-infinite "body" created by a particular axial source distribution so that a surface pressure distribution could be calculated.

(e) a 3in diameter disc set normal to the stream (plate 8).

2. SURFACE APPEARANCE OF CAVITIES

For each of the five headforms photographs of both natural and ventilated cavities were taken at a series of tunnel velocities, U_T, the tunnel pressure taking roughly its lowest operational value in all cases. It was apparent not only in the photographs but also to the naked eye that the appearance of the cavity surface was markedly different depending on whether the cavity was or was not filled with the turbulent froth of bubbles and water associated with the re-entrant jet. Although clearly there were intermediate states of incomplete filling the observed characteristics of the extreme cases will be described first.

Plates 1 and 2 represent examples of the former type, referred to as being partially developed and confined almost exclusively to the natural cavity flows. Ventilation seemed to produce either a train of bubbles from the exit holes or a fully developed cavity flow (as defined below) with virtually no intermediate state. The following observations seemed generally applicable to the "filled" cavities:

(i) The ogive and the cut-away sphere, headforms with a sharp, separating edge, produced "filled" cavities typified by plate 1. The characteristic gap of clear water between the base of the headform and the cavity is a somewhat surprising feature. In other photographs the gap may not have extended right to the centre of the base but always appeared near its periphery. The irregularities of the surface of the cavity do seem on examination to contain a characteristic frequency or wavelength which may be associated with a vortex shedding frequency from the sharp trailing edge of the headform (these frequencies are considerably larger than those discussed in the later part of the paper).

(ii) Under the same conditions the two spheres with no sharp "separating" edge producedpartially developed cavities which were much less steady (plate 2 being a typical example) and could be adequately described as being in an advanced state of incipient cavitation.

For convenience in the context of this paper a fully developed cavity is defined as one in which the flow separates (in the cavitation sense) along a well defined line on the surface of the headform to produce a cavity which is not filled with bubbles. The filling effect of the re-entrant jet decreases with increasing cavity length. It was incidentally observed that the "strength" and penetration of the jet within a natural cavity was noticeably greater than for a ventilated cavity under identical conditions of tunnel velocity and cavity length. This may be associated with the different mass rates of vapour and gas entrainment into the wake as discussed in an earlier paper (Brennen (1968b)). Whenever the jet impinged on the cavity wall the latter became rough, unsteady and opaque as in the bottom left-hand corner of plate 3.

Attention will now be focused exclusively on the nature of cavity surfaces which are unaffected by such interference. The singular appearance of the interface just downstream of separation was first noted in photographs of the 3 in sphere, plate 3 being a typical example. Immediately following separation the surface is smooth and glassy. Downstream of this a system of waves with crests running perpendicular to the direction of flow appears to be imposed on the clear surface. Moving with the fluid these waves presumeably grow in amplitude until they break up to form the rough or turbulent surface which persists along the length of the cavity. The naked eye could detect the two regions of smooth and

turbulent surface though not the intervening wave pattern. Also visible in the case of the 3 in sphere were the longitudinal striations which especially near separation, tended to disturb the described pattern (see plate 3). These striations were caused by small drops of water (from condensation or the spray of the re-entrant jet) being trapped in the very thin cavity just after separation. The drops and associated striations continually moved downwards under the influence of gravity. No such thin cavity region occurs with the cutaway sphere or ogive and hence as can be seen from plates 4 and 5, there are no striations. Similar, but fixed, striations on the cavity surface may however be caused if there were any irregularities in the headform at or near separation (Gadd and Grant (1965)).

3. FURTHER OBSERVATIONS OF THE WAVE PATTERNS

The most plausible explanation of the appearance of the wave patterns lies in the nature and behaviour of the boundary layer on the wetted surface up to separation and following separation where it becomes a free surface boundary layer. Comparison of theory and experiment in section 6 seems to confirm that the waves are the amplified result of a selected frequency instability of the classical Tollmein Schlicting type in the boundary layer. The question arises as to whether the original instability and therefore the determination of the frequency which is amplified occurs in the laminar boundary layer before or after separation. The theoretical considerations of the following sections suggest that the instability follows separation though clearly the neccessary "noise" required to excite it may find its source in headform surface roughness, very small amplitude instability in the attached boundary layer or other imperfections in the flow.

The boundary layer on the wetted surface of the 3 in sphere evidently remains laminar even at the highest velocity (45 ft/sec) or a Reynolds number based on tunnel velocity, U_T, and sphere diameter, D, of about 9.5×10^5. In non-cavitating flow past a sphere the boundary layer becomes turbulent and its separation shifts to a position downstream of the equatorial line above a Reynolds number of about 2.5×10^5. Clearly, the effect of the cavity and the associated early separation is to maintain a wholly laminar boundary layer on the wetted surface to well above this figure.

Fully developed cavities could be created at tunnel speeds as low as 10ft/sec by using the ventilation available. Provided a fully developed cavity could be established, whether it was ventilated or natural made no apparent difference to the wave pattern phenomenon at a particular tunnel velocity, U_T. In fact the wavelength, λ, and the width of the smooth region seemed unaffected by cavity or tunnel pressure and varied only very slightly with cavitation number, σ, within the relevant range (approx. $0.1 < \sigma < 0.4$); however both lengths substantially increased with decreasing tunnel velocity, U_T. Apart from the minor differences

outlined below, the same remarks apply to the wave patterns found with the ogive, cut-away sphere and $1_{1/8}$ in sphere (plates 4 to 7).

Transition to turbulence occured on the surface of cavities behind the ogive (plate 4) at all the tunnel speeds investigated. However with the 3 in and cut-away spheres the point of break up of the wave pattern moved downstream as U_T was decreased to about 14 ft/sec, below which velocity this transition ceased to occur and the waves persisted along the length of the cavity as in plate 6. It may be observed in this figure that the wave crests become progressively more inclined to the vertical (or back face of the cutaway sphere) with increasing distance from separation. This was due to the slight variation of cavity surface velocity with vertical elevation or dynamic water head, the cavity pressure being uniform. If U_w denotes the mean wave crest velocity then the rate of increase of the inclination (at the centre of the side of the cavity) with horizontal position, $d(\tan\theta)/dX$, should be g/U_w^2. Measurements from plate 6 of the inclination, $\tan\theta$, are plotted against distance from separation, X, in figure 1. The fluid velocity on the interface will asymptote from zero at separation to $U_T\sqrt{1+\sigma}$ or 12.8 ft/sec (the theoretical potential flow velocity of the free streamline). The slope of the full Line of figure 1 indicates a wave crest velocity of 12.6 ft/sec, virtually identical with the fluid velocity. The dotted line is a tentative continuation assuming that the original infinitesmal disturbance has a vertical crest line at separation; such a curve would be consistent with U_w increasing from its separation value to $U_T\sqrt{1+\sigma}$ by the time the disturbance had reached finite amplitude proportions.

High speed cine films (~4000 frames/sec) were taken of the wave patterns in flows similar to those of plates 3, 5 and 6. A study of successive frames confirmed that to within the order of accuracy of measurement, the crest velocity of the finite amplitude waves was equal in all cases to what potential flow theory would predict for the fluid velocity on the interface, namely $U_T\sqrt{1+\sigma}$.

In the case of the $1_{1/8}$ in sphere full transition ceased to occur below about about 17 ft/sec (plate 7). The wave patterns were not quite so remarkably regular as in the earlier cases possibly due either to the relatively larger wavelength or to the disturbance caused by the ventilation air which is emitted radially rather than in the downstream direction of the other headforms.

But the last headform, the 3 in disc, gave completely clear cavities (as in plate 8) at all the possible tunnel velocities with no sign of a wave pattern. Some tests were carried out to determine whether by artifically increasing the noise level in the boundary layer of the disc an instability could be excited. Plates 9 and 10 were the results of two such attempts, all of which were inconclusive since frequencies of vortex shedding from the disturbers (a row of pegs in plate 9; a square section ring in plate 10) may be reflected in the

free surface. However, the case of the disc is further discussed in section 6 following the theoretical study of the stability of a separated free surface boundary layer.

The measurements from the photographs of the wavelength, λ, of the finite amplitude waves are plotted non-dimensionally in figure 2, D being the diameter of the sphere or of the base of the ogive and U_T the tunnel velocity (thus $U_T D/\nu$ is a conventional Reynolds number). The propagation velocity of the waves has been seen to be virtually equal to $U_T\sqrt{1+\sigma}$ and hence the frequency of the disturbance generating the waves could be computed in each case (see section 6). The distance from separation to the break up of the wave pattern or appearance of turbulence, X_1, is plotted in figure 3. Although this measurement, especially in the case of the ogive, was somewhat arbitrary a study of the profile of the surface enabled a fair estimate to be made.

4. THEORY OF THE INSTABILITY OF THE INTERFACIAL BOUNDARY LAYER

A number of simplifications are required to provide a mathematical model, amenable to theoretical computation, of the boundary layer flow through and following separation. Since the boundary layer thickness is minute compared with both the distance of the separation point from the axis and the longitudinal radius of curvature of the cavity surface and since in all but the case of the disc headform the flow in this region is not far from parallel with the axis it seemed that a reasonable approximate mathematical model would be the planar flow of figure 4. It was further assumed that the momentum thickness, δ_2, of the interfacial boundary layer remained unaltered after separation. Then the following notation is used to describe the mean flow:

X,Y physical coordinates shown in figure 4, the origin of X,Y being the separation point.

T time.

$x = \dfrac{X}{\delta_2}$, $y = \dfrac{Y}{\delta_2}$, $t = \dfrac{U_\infty T}{\delta_2}$ Nondimensional coordinates.

U_∞, u, U_c physical velocities; of the uniform stream, at a point in the layer and on the line $y = 0$.

$w = (U_\infty - u)/U_\infty$

w_c The function $w_c(x) = (U_\infty - U_c)/U_\infty$. Then $w_c = 1$ at separation and tends to zero downstream

B A half-breadth of the boundary layer, i.e. $Y = B$, $w = \frac{1}{2}$

b The function $b(x) = B/\delta_2$.

Since the tangential stress is taken to be zero on the free streamline, $Y = 0$, the flow model will then be identical to that for half the flow in the wake of a thin flat plate set parallel to a uniform stream.

The stability of the flow within the boundary layer will be investigated following conventional linearized procedure. To study the stability at a particular x position, the velocity distribution at that position is considered as describing a mean flow which is invariant in the x direction with a perturbation stream function, ψ, of the form:

$$\psi = \phi(y) \exp [i \alpha_{\delta_2} (x-ct)]$$

where α_{δ_2} = the dimensionless wave number of the disturbance, $\alpha \cdot \delta_2$, α being the physical wave number $= \frac{2\pi}{\lambda}$

$c = c_r + i\, c_i$

c_r = non dimensional propagation velocity based on U_∞

c_i = a measure of the rate of amplification of the disturbance.

Also $R_{\delta_2} = U_\infty \cdot \delta_2/\nu$ where ν is the kinematic viscosity.
Then ϕ must satisfy the Orr-Sommerfeld equation

$$\left(\frac{u}{U_\infty} - c\right)\left(\frac{\partial^2\phi}{\partial y^2} - \alpha_{\delta_2}^2 \phi\right) - \phi \cdot \frac{\partial^2}{\partial y^2}\left(\frac{u}{U_\infty}\right) = \frac{-i}{\alpha_{\delta_2} R_{\delta_2}}\left(\frac{\partial^4\phi}{\partial y^4} - \frac{2\alpha^2\partial^2\phi}{\partial y^2} + \alpha^4 \phi\right) \quad \ldots [1]$$

Since the form of the velocity distribution function, $\frac{u}{U_\infty}$, changes with position x and with Reynolds number R_{δ_2} the required solution would involve a knowledge of that velocity distribution (Goldstein's (1933) detailed analysis in the wake of a flat plate could be employed) and the computation and tabulation through equation [1] of the eigenvalues in the form, say, of c_i and c_r plotted against α_{δ_2} for every x position for the required series of Reynolds number. But only the theoretical, inviscid solution and a slight modification of it have been attempted here. Moreover the velocity distribution has been assumed to take the Gaussian form:

$$\frac{w}{w_c} = e^{-(\ln 2)\left(\frac{y}{b}\right)^2} \quad \ldots [2]$$

which leads to considerable simplification but is only, in fact, applicable in a viscous solution sufficiently far downstream of separation (Goldstein (1933)). Substituting into equation [1] and re-organizing:

$$\left(\frac{w}{w_c} - k\right)(\phi'' - \alpha_B^2 \phi) - \left(\frac{w}{w_c}\right)'' \phi = \frac{i}{\alpha_B R_B^*}(\phi'''' - 2\alpha_B^2 \phi'' + \alpha_B^4 \phi) \quad \ldots [3]$$

where:

$$k = (1-c)/w_c = k_r + i\,k_i$$
$$\alpha_B = b \cdot \alpha_{\delta_2} \qquad \ldots [4]$$
$$R^*_B = b \cdot w_c \cdot R_{\delta_2}$$

and dashes denote differentiation with respect to $\left(\frac{y}{b}\right)$ or $\left(\frac{Y}{B}\right)$. Since $\frac{w}{w_c}$ varies from 1 to zero across the shear layer it is simpler to work with [3] rather than [1] whose eigenvalues depend upon the particular value of w_c.

Boundary conditions required for the solution of the eigenvalue problem are:

$\phi_{y=0} = 1$	Sets the scale of ϕ
$\phi'_{y=0} = 0$	The condition of zero shear stress or vorticity on the free surface in linearized theory.
$\phi'_{y=\infty} + \alpha_B\,\phi_{y=\infty} = 0$	The usual condition taken to apply at infinity (Rosenhead (1966)).

For the inviscid solution the right hand side of equation [3] was replaced by zero and numerical integrations, using the Runge-Kutta procedure, were performed along a contour in the complex plane of y (avoiding possible singularities at the critical point) in order to compute the eigenvalues α_B, k_r and k_i. The results are shown by the full lines in figure 5. Using a Gaussian distribution with equation [1], Sato and Kuriki (1961) computed inviscid eigenvalues for the case $w_c = 0.692$ in connection with the flow in the wake of a flat plate. Converting their results for c to values of k using $w_c = 0.692$ yields the broken lines in figure 5. There would seem to be marked disagreement in the results for k_i at smaller α_B, which may be due to the limited computer space which Sato and Kuriki had available combined with their use of the "c-equation", [1], rather than the "k-equation", [3].

Using an approximation to the Gaussian distribution, McKoen (1955) performed neutral stability (i.e. $k_i = 0$) computations on equation [3] for $R^*_B \neq \infty$ but neglecting the ϕ''''term. But as mentioned above a non-infinite Reynolds number would also alter the form of the distribution [2]. An approximate estimate of the former of these two effects can be obtained by retaining the right hand side of [3] except for the difficult ϕ''''term and solving for a number of values of R^*_B. The range of R^*_B that needs to be considered is not unduly large since from equation [2] and the definition of momentum thickness

$$\frac{1}{b} = \sqrt{\frac{\pi}{4 \ln 2}}\left[w_c - \frac{w_c^2}{2}\right] \qquad \ldots [5]$$

Thus from the last of equations [4] it is easily seen that R^*_B depends mainly on R_{δ_2} and only to a limited extent on position x which governs w_c. Values of

k_i obtained for the particular case $R^*_B = 50$ are plotted in figure 5, the k_r line being virtually indistinguishable from the inviscid result.

5. GROWTH OF THE DISTURBANCE IN THE SEPARATED LAYER

The frequency of the disturbance, f, and a non-dimensional frequency, γ, are given by

$$\gamma = 2\pi f \cdot \frac{\delta_2}{U_\infty} = \alpha_{\delta_2} \cdot c_r = \frac{\alpha_B}{b}\left[1 - k_r \cdot w_c\right] \qquad \ldots [6]$$

In the time dependent eigenvalue solution of the last section the disturbance grows in amplitude according to $\exp(\alpha_{\delta_2} c_i t)$. But the wave crests move downstream with speed c_r, so the transformation $x = c_r t$ relates time to position and in the actual flow where wave amplitudes are functions only of position, the amplitude grows like $\exp(\alpha_{\delta_2} c_i x/c_r)$. If A denotes the general amplitude and A' the spatial rate of amplification then

$$\frac{1}{A}\frac{\partial A}{\partial x} = \frac{A'}{A} = \frac{\alpha_{\delta_2} c_i}{c_r} = -\frac{\alpha_B}{b} \cdot \frac{w_c k_i}{\left[1 - k_r w_c\right]} \qquad \ldots [7]$$

At a particular x position the frequency, γ, or wave number, α_B, which gives the maximum rate of amplification will be given from equation [7] by the solution of

$$1 + \frac{\alpha_B}{k_i}\frac{\partial k_i}{\partial \alpha_B} + \frac{\alpha_B}{\left[\frac{1}{w_c} - k_r\right]}\frac{\partial k_r}{\partial \alpha_B} = -\frac{\alpha_B}{A} \cdot \frac{\partial A}{\partial \alpha_B} \qquad \ldots [8]$$

Then the results of figure 5 enable the values of γ and α_B for maximum amplification to be calculated for various values of w_c and for $\partial A/\partial \alpha_B = 0$. Also shown in figure 6 are the Reynolds number modified results for $R_{\delta_2} = 50$ and the frequencies of neutral stability, $A' = 0$, the computation of which required the use of the functions $b(w_c)$ and $R^*_B(w_c)$ and the relation [5]. The dimensionless velocity deficit on the free surface, w_c, starts with a value of unity at separation and asymptotes to zero with increasing distance from separation. In the present context it is convenient to use the variable w_c to give some indication of position, x, on the free surface. Typically it requires a distance of several hundred (or R_{δ_2}) momentum thicknesses to reduce w_c to $\frac{1}{2}$.

As in other problems of boundary layer instability one frequency is preferred and amplified to the virtual exclusion of all others. Since the growth of amplitude is exponential it is clear that dominance of a particular frequency is likely to be increased as the disturbance is convected downstream. If the noise in the boundary layer up to and at separation ($w_c = 1$) were white (i.e.

$\partial A/\partial \alpha_B = 0$) then, from figure 6, a frequency, γ, in the range $0.266 \rightarrow 0.290$ would clearly achieve initial dominance at large Reynolds numbers. This disturbance would then be amplified as it moved downstream (decreasing w_c) until neutral stability was reached, following a horizontal line in figure 6. If by that time the disturbance reached finite amplitude proportions the waves would thereafter tend to be damped, providing that break up into turbulence did not occur before that point. Non-linear or second order effects due to the finite amplitudes will have a quantitative though not qualitative influence on these later behaviour patterns.

Similarly a frequency in the range $0.256 \rightarrow 0.277$ is likely for $R_{\delta_2} = 50$ according to the Reynolds number modified solution. These ranges of γ are shown in figure 7 in which experimental frequencies, discussed below, are plotted against R_{δ_2}.

6. INTEGRATED AMPLIFICATION

In order to obtain some estimate of the total amplification undergone by the disturbance to reach finite amplitude proportions and turbulent break-up it is necessary to integrate equation [7]. If for a given frequency, γ, A_s and A denote the amplitudes of the noise at separation and of the disturbance at position x then:

$$\ln\left(\frac{A}{A_s}\right) = \int_0^x -\frac{\alpha_B^2 \cdot k_i \cdot w_c}{b^2 \cdot \gamma}\, dx \qquad \ldots [9]$$

Through equations [5] and [6] b, α_B and k_i are known functions of w_c for the given frequency, γ. To perform the integral requires then a knowledge of the function $w_c(x)$ which has, as yet, been unneccessary. Goldstein's (1933) result can be re-written as

$$w_c = z^{\frac{1}{2}} + \frac{z}{2} \quad \text{where} \quad z = \frac{R_{\delta_2}}{\Pi(x + x_0)} \qquad \ldots [10]$$

and x_0, the virtual origin of the separated layer, will be given by $w_c = 1$, $x = 0$. By virtue of this relation, the choice of Reynolds number will have a dominant effect on the integral [9]. This dependence will clearly overshadow the deviation of the functions $b(w_c)$, $\alpha_B(w_c)$ and $k_i(w_c)$ from their inviscid form to their form for finite R_{δ_2}. Thus as a first approximation at least the inviscid form of these functions was used in conjunction with equation [10] to compute $\ln\left(\frac{A}{A_s}\right)$ as a function of x for particular frequencies and Reynolds numbers. In figure 8, a graph of x position against R_{δ_2}, the lines of constant $\ln\left(\frac{A}{A_s}\right)$ for particular frequencies were plotted from these calculations. It has however to be noted that non-linearity due to the finite amplitudes may have a significant effect on these results.

7. COMPARISON OF THEORY AND EXPERIMENT

In order that the experimental results for the various headforms may be correlated and compared with theory some estimate of the momentum thickness at separation, δ_2, is clearly required for each of the axisymmetric headforms. For this purpose the integral method of Rott and Crabtree (1952) was used in conjunction with theoretical wetted surface pressure distributions for the sphere and disc obtained in a previous paper (Brennen (1968a)) and for the ogive from the source distribution from which that headform was designed. Then

$$\delta_2 = I\sqrt{\frac{D\nu}{U_T}}$$

where D is the maximum diameter of the body and $I \approx 0.29$, 0.061 and 0.746 for the sphere, disc and ogive respectively. But as was shown in the paper just cited the actual separation point in the case of the sphere is some distance downstream of that predicted by theory. In order to allow for the effect of this on I the pressure distribution was extended by a constant pressure between the two separation positions. The modified values for I were 0.30 for the cutaway sphere, 0.31 for the 3 in sphere and 0.34 for the $1_{1/8}$ in sphere.

Thus δ_2 and R_{δ_2} corresponding to each point of figures 2 and 3 were calculated and values of γ (computed through the definition [6] where f is found as indicated at the end of section 3) and $\frac{X_1}{\delta_2}$ plotted in figures 7 and 8 respectively.

Results for experimentally observed frequencies in the wake of a thin flat plate are shown in figure 7. Those of Hollingdale (1940) and Taneda (1958) in which the fluid is water have been non-dimensionalized using the formula, $\delta_2 = 0.664\sqrt{\frac{\nu L}{U_T}}$. Sato and Kuriki's (1961) results (in air) for $\alpha_B\, c_r$ at $w_c = 0.692$ have been converted using equation [5] since their measured velocity distribution at that point is virtually Gaussian.

All the results seem to indicate an asymptotic inviscid solution very close to the range predicted by theory. However the Reynolds number modification of sections 4 and 5 is clearly insufficient. Although some doubt must persist due to the neglect of the ϕ'''' term it is suggested that the influence of finite R_{δ_2} on the function $\frac{w}{w_c}$ is probably more important than its effect on the R.H.S. of equation [3]. The velocity distribution will change from near-Blasius some distance upstream to near-Gaussian some distance downstream of separation. As the Reynolds number is reduced, the results of Goldstein, Hollingdale and others suggest that the distribution at and shortly after separation tends further toward the former type and thus the instability frequency is correspondingly reduced towards that for a Blasius distribution, for which the theoretical neutral stability curve due to Lin (1945) is shown in figure 7.

The flat plate results in which the scatter on both "mean" lines is about ± 0.02 in γ lie somewhat above those from the present experiments. The results for the spherical headforms may be affected by the axisymmetric divergence of the interface and the corresponding reduction in δ_2 with distance from separation.

The theory does not suggest the existence of a critical Reynolds number below which all frequencies are stable. The absence of finite amplitude waves in the case of the disc (whose range of R_{δ_2} is shown in figure 7) does not preclude the existence of unstable frequencies in that range. It seems likely from an extrapolation of the results for the other headforms to the low R_{δ_2} of the disc experiments that any disturbances present there would have low frequencies and corresponding low amplification rates. Accordingly the much larger axisymmetric divergence and longitudinal curvature of the interface in this case probably prevent sufficient growth to produce finite amplitude waves before the neutral stability position is reached (see below).

When the disturbances reach finite amplitude proportions not only will linearized theory become less accurate but the waves will also be subject to the effects of surface tension and the centrifugal acceleration due to the longitudinal curvature of the interface. A parallel may thus be drawn with gravity/capillary waves on a horizontal free surface. Turbulence may first occur when the amplitude reaches a critical size and the waves "break" in the conventional manner. Despite the innacuracies of measurement figure 8 would suggest that for each headform break up occurs very roughly along a line of constant total amplification indicating that if the noise level in the attached boundary layer (A_s) were roughly independent of R_{δ_2}, the waves would break on reaching a critical amplitude.

However below a particular value of R_{δ_2} (given by the neutral stability point of lines such as A,B,C,D) the necessary amplification is not acheived and the waves continue without break up. Surface tension and acceleration may constrain amplitude growth to a certain extent so that the neutral stability position may be upstream of that predicted by theory.

8. CONCLUDING REMARKS

This paper continues the author's series of papers dealing with effects of the boundary layer on cavitating flows. The effect on the position of separation was discussed in an earlier paper (Brennen (1968a)). In another previous paper (Brennen (1968b)) the existence of a turbulent boundary layer on the surface of the cavity was shown to increase dramatically the expected and actual partial pressure of air in the cavity when the water contains dissolved air, resulting in a decrease in drag on the headform.

The main concern of the present paper is to describe and account for the ripples or waves observed on the cavity surface just downstream of separation. Stability theory applied to the separated and initially laminar boundary layer suggests that the waves are the finite amplitude result of excited instabilities in this layer. Thus the measured frequencies are compatible with those obtained in the theory where the selected frequency is that which has the maximum spatial rate of amplification at or immediately following separation. Under some conditions the waves break up yielding a turbulent interfacial layer and the points at which this occurs for a particular headform appear to lie close to a line of constant total amplification. Under other conditions the point of neutral stability is reached before sufficient amplification for break up has been achieved and the waves continue along the length of the cavity. With one of the headforms, the disc, no wave patterns were observed; some attempt to explain this is made in section 7.

10. ACKNOWLEDGEMENTS

This work is part of the research programme of the Ship Division of the National Physical Laboratory. The author wishes to thank Mr. S. Grant for assistance in carrying our the experimental investigations, Dr. A. Davey (Aerodynamics Division) for extensive aid in the computer program for the solution of the eigenvalue problem and Dr. G.E. Gadd for valuable discussions on the subject.

REFERENCES

1. BRENNEN, C. 1968a A Numerical Solution of Axisymmetric cavity flows. Parts I and II. N.P.L. Ship Division Report, No. 114.

2. BRENNEN, C. 1968b The Dynamic Balances of Dissolved air and heat in natural cavity flows. N.P.L. Ship Division Report, No. 115.

3. GADD, G.E. and GRANT, S. 1965 Some experiments on cavities behind disks. J. fluid Mechs., 23, 4.

4. GOLDSTEIN, S. 1933 On the two-dimensional steady flow of a viscous fluid behind a solid body. Proc. Roy. Soc. A, 142.

5. HOLLINGDALE, S.H. 1940 Stability and configuration of the wakes produced by solid bodies moving through fluids. Phil. Mag. (7), 29.

6. LIN, C.C. 1945 On the stability of two-dimensional parallel flows. Quart. appl. Math., 3.

7. McKOEN, C.H. 1955 Stability of laminar wakes. Current Papers aero. Res. Cam. Lond., No. 303.

8. ROSENHEAD, L. 1966 Laminar Boundary Layers, Oxford University Press.

9. ROTT, N. and CRABTREE, L.F. 1952 Simplified laminar boundary layer calculations for bodies of revolution and for yawed wings. J.aero. Sci., 19.

10. SATO, H. and KURIKI, K. 1961 The mechanism of transition in the wake of a thin flat plate placed parallel to a uniform flow. J.fluid Mechs., 11.

11. TANEDA, S. 1958 Oscillation of the wake behind a flat plate parallel to the flow. J. phys. Soc. Japan, 13, 4.

9th August 1968
BM

FIG. 1.

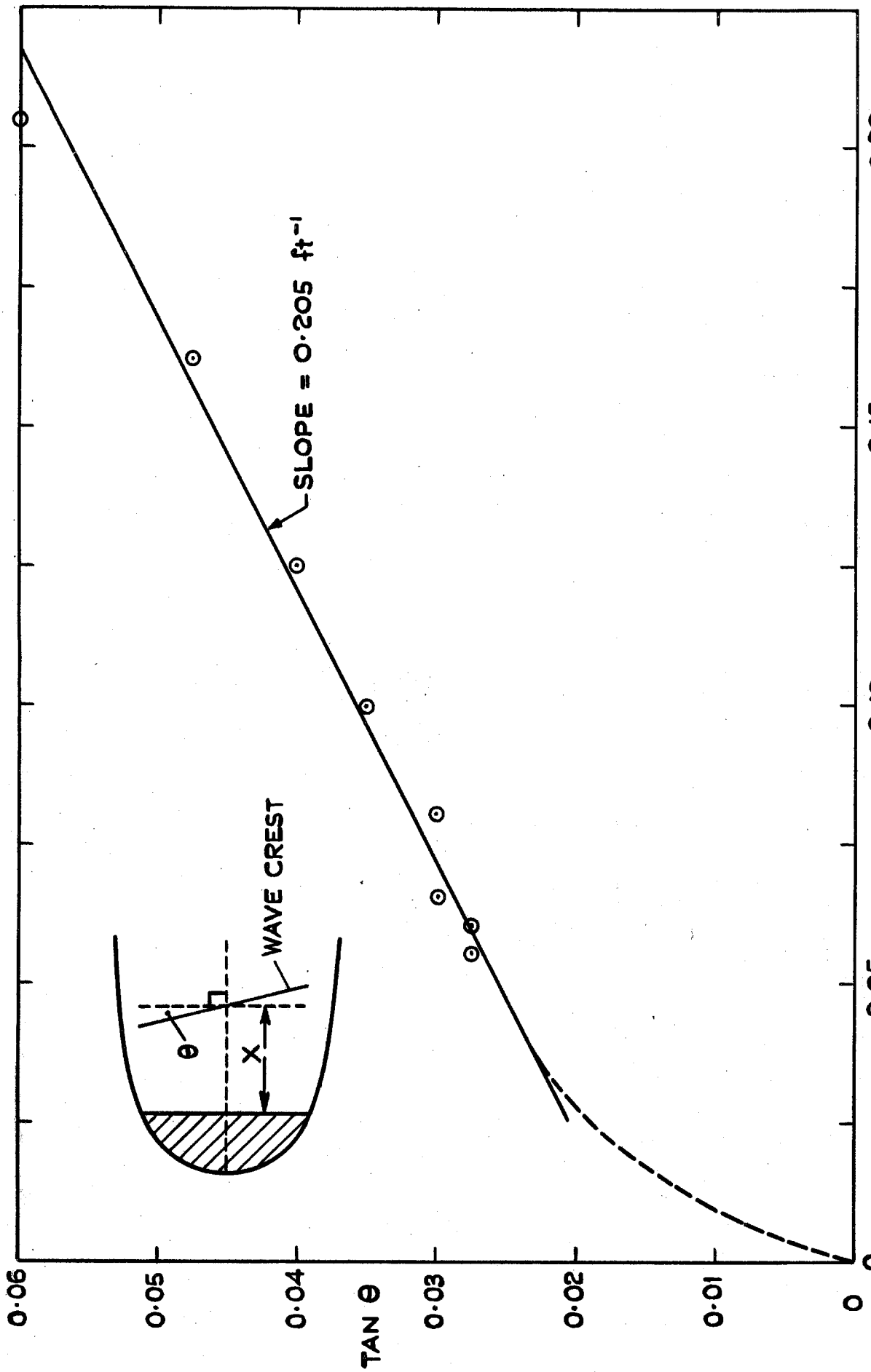

FIG.1. X – VARIATION OF WAVE CREST INCLINATION TO VERTICAL

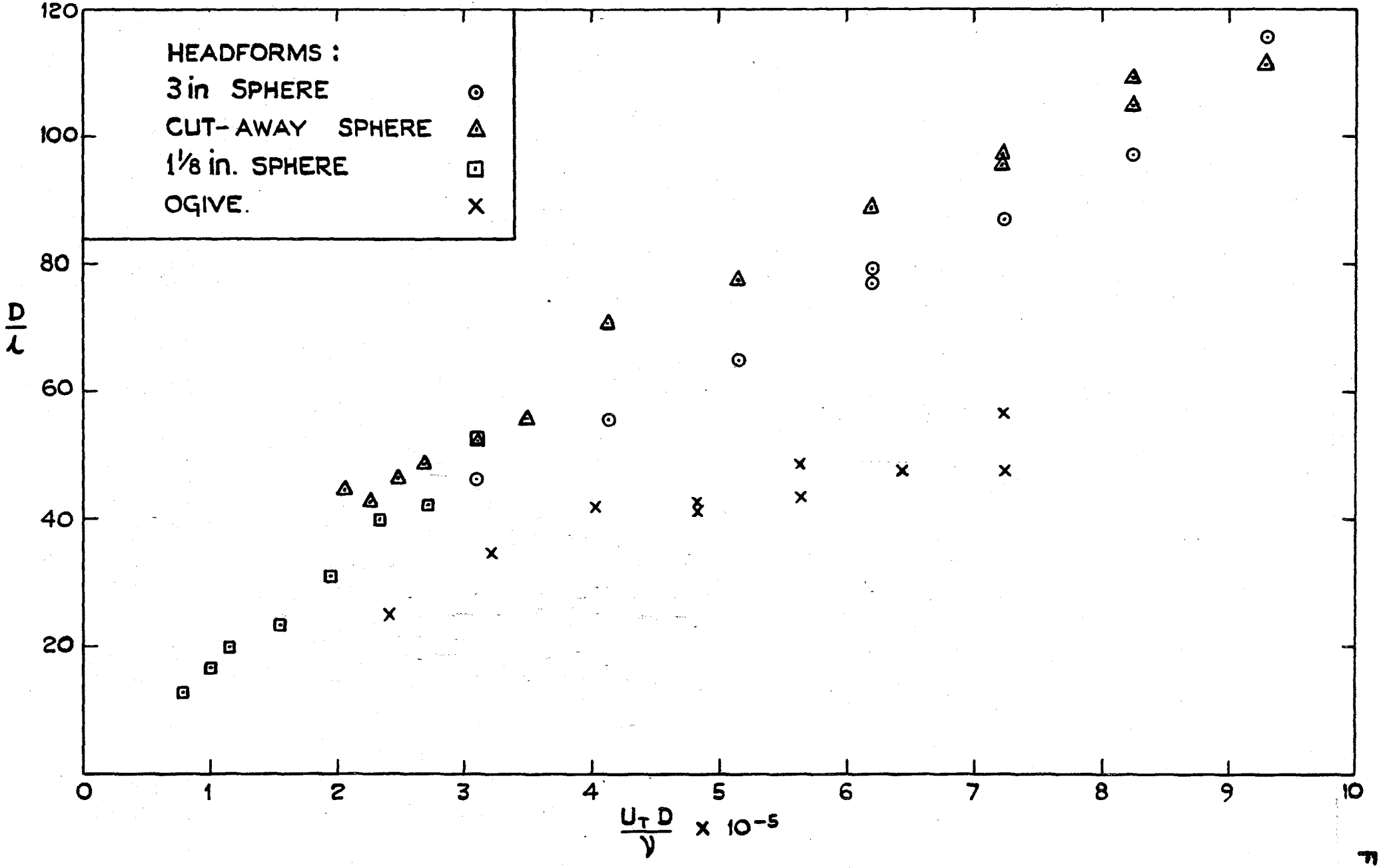

FIG. 2 VARIATION OF WAVELENGTH, l, WITH TUNNEL VELOCITY, U_T

FIG. 2.

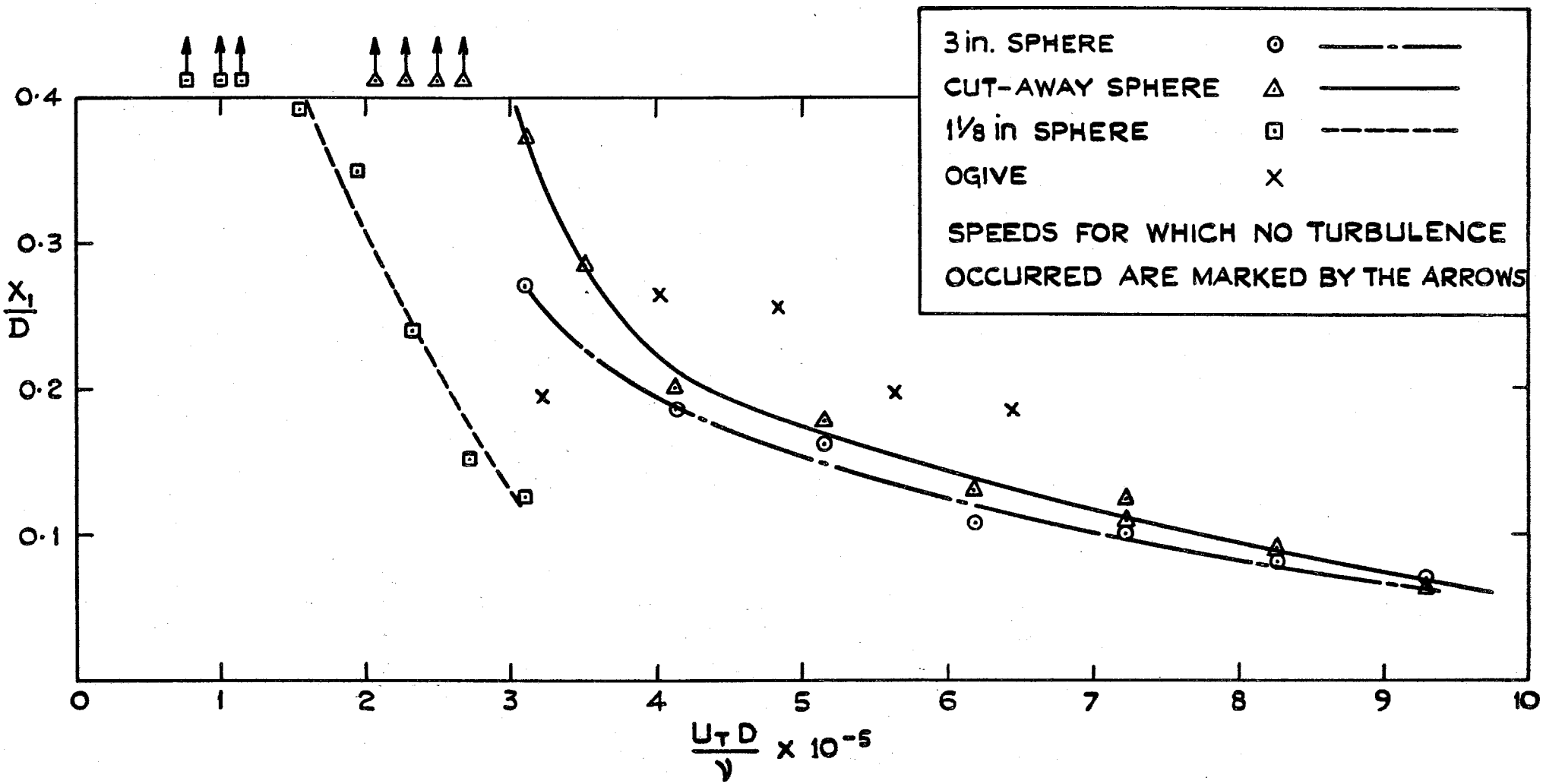

FIG. 3. VARIATION OF DISTANCE TO WAVE BREAK UP WITH TUNNEL VELOCITY, U_T

FIG. 3.

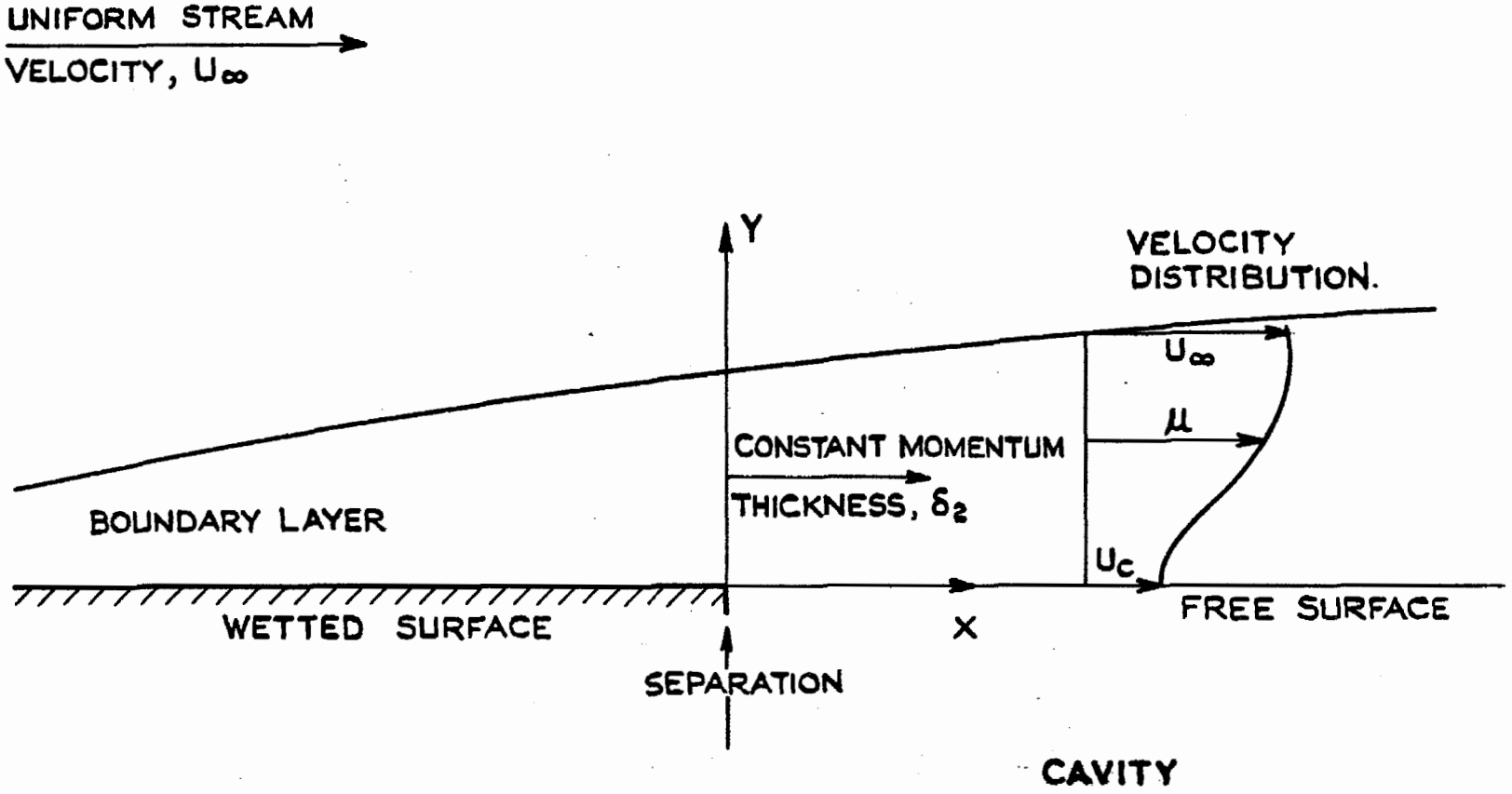

FIG. 4. MATHEMATICAL MODEL OF BOUNDARY LAYER FLOW NEAR SEPARATION

FIG. 4

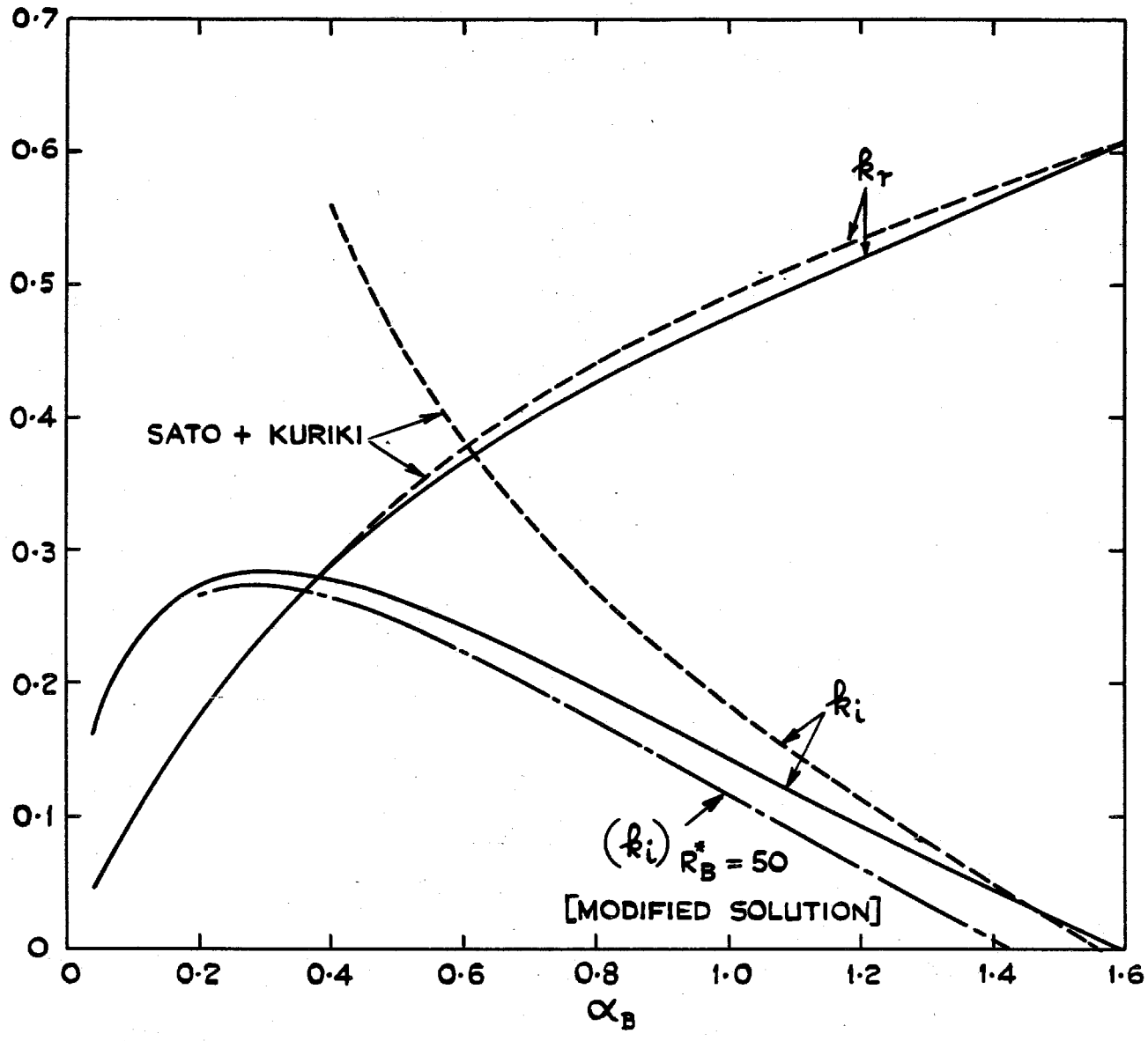

FIG. 5. EIGEN VALUE SOLUTIONS OF THE STABILITY EQUATION

FIG. 5.

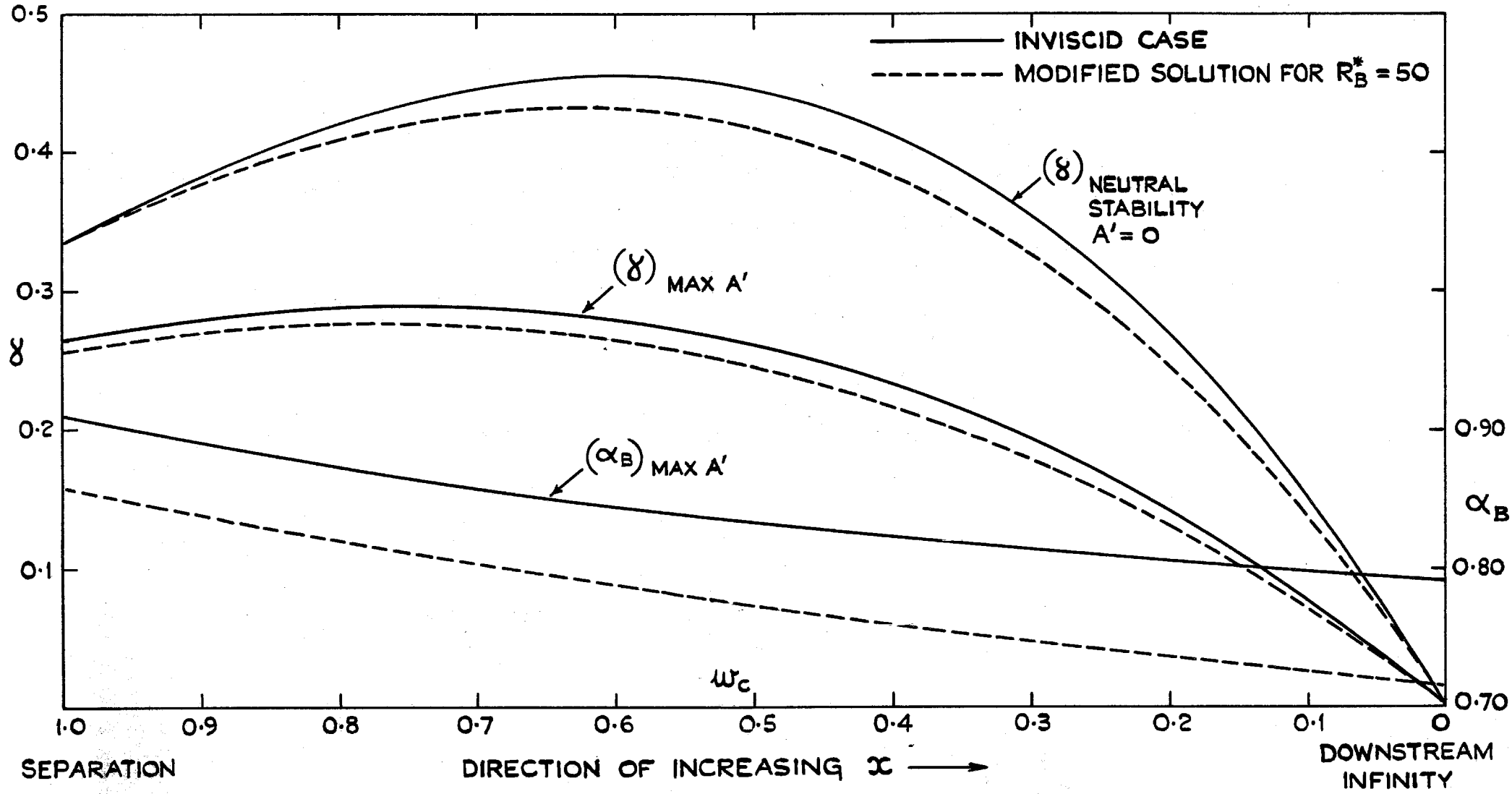

FIG. 6. MAXIMUM GROWTH RATE AND NEUTRAL STABILITY FREQUENCIES AS FUNCTIONS OF ω_c

FIG.6.

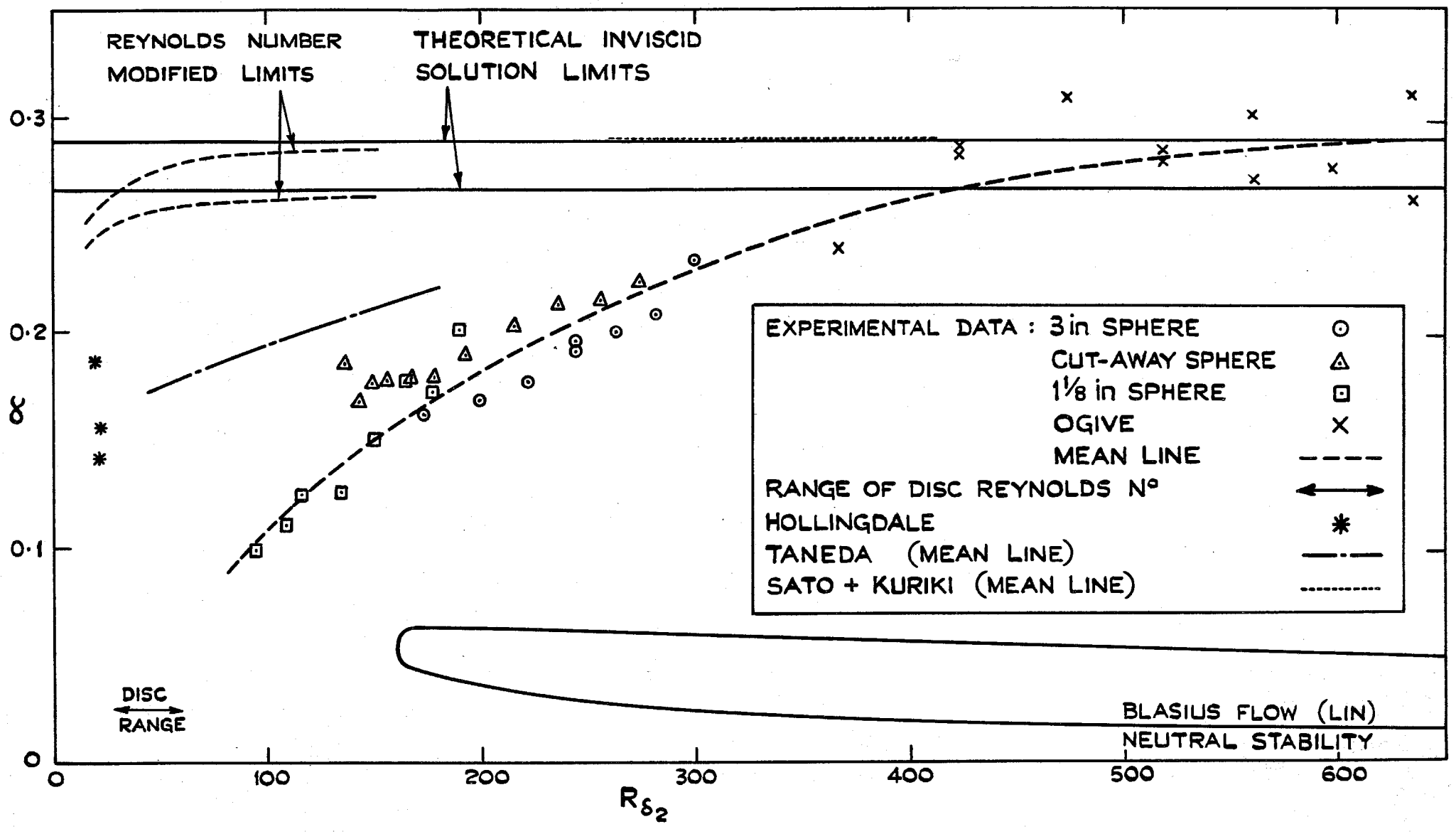

FIG. 7.

FIG 7. NON-DIMENSIONAL INSTABILITY FREQUENCY AGAINST REYNOLDS NUMBER

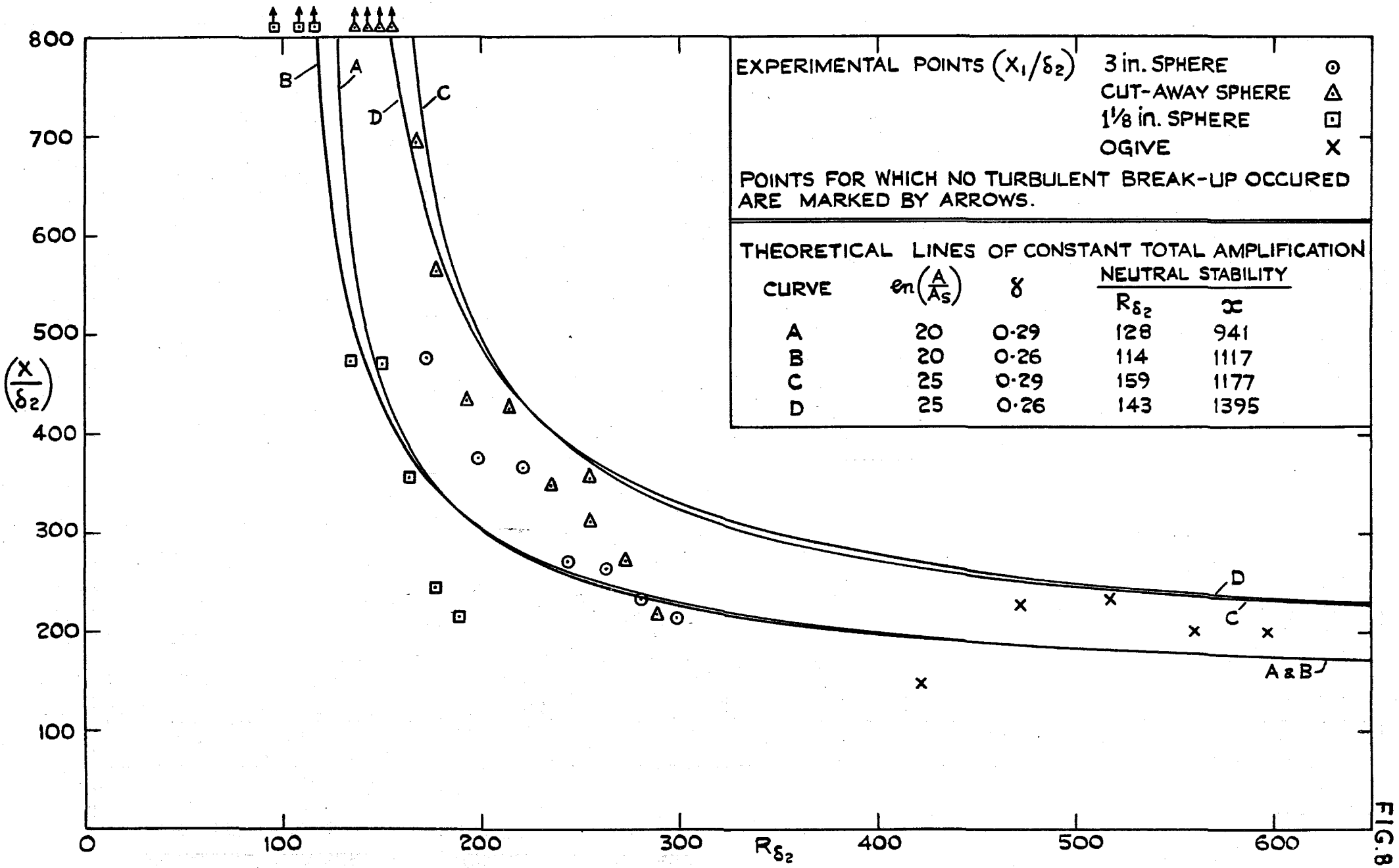

FIG. 8. NON-DIMENSIONAL DISTANCE TO WAVE BREAK-UP COMPARED WITH THEORETICAL LINES OF CONSTANT TOTAL AMPLIFICATION

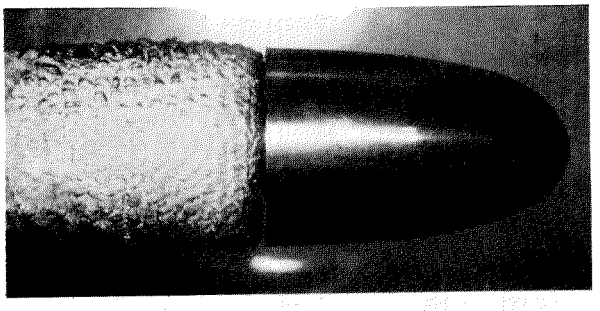

Plate 1. Ogive. U_T = 30 fps.
Natural cavity.

Plate 2. 3 in. Sphere. U_T = 20 fps.
Natural cavity.

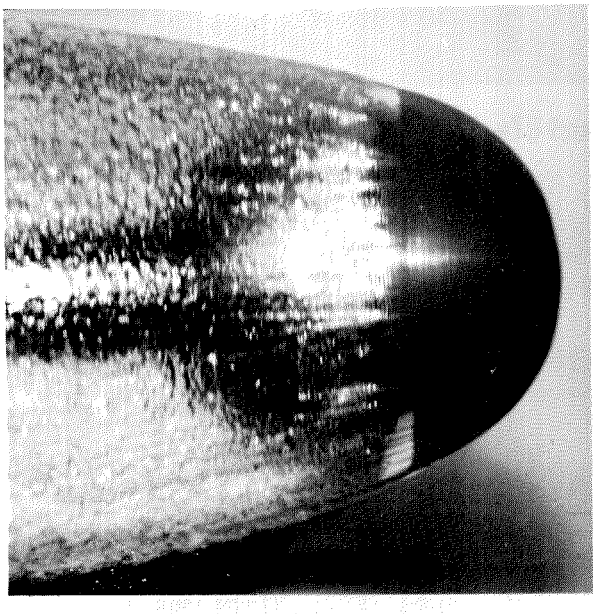

Plate 3. 3in. Sphere. U_T = 35 fps.
Natural cavity.

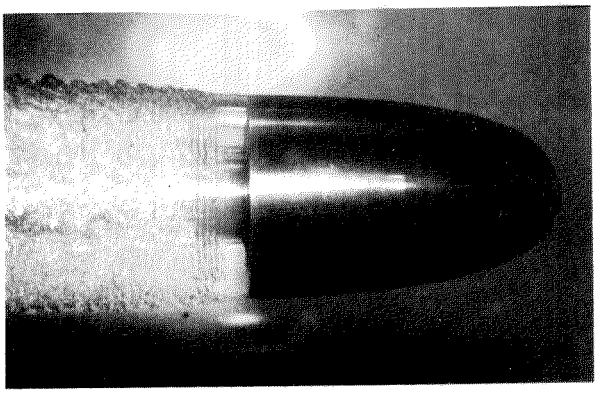

Plate 4. Ogive. U_T = 25 fps.
Ventilated cavity.

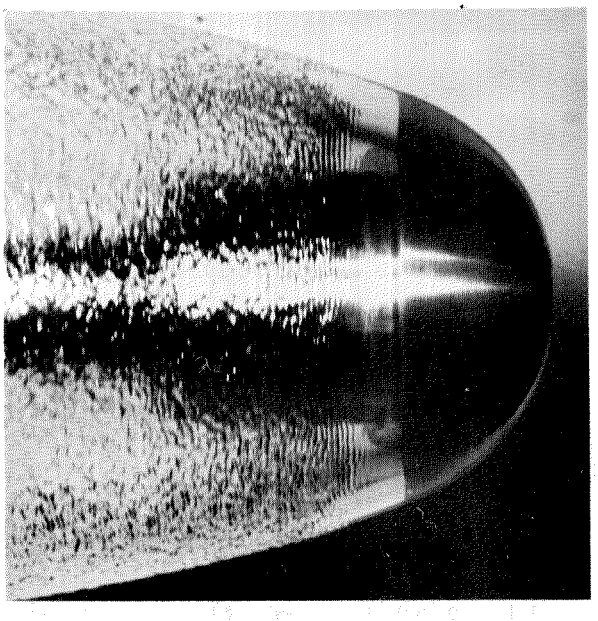

Plate 5. Cut-away Sphere.
Ventilated. U_T = 20 fps.

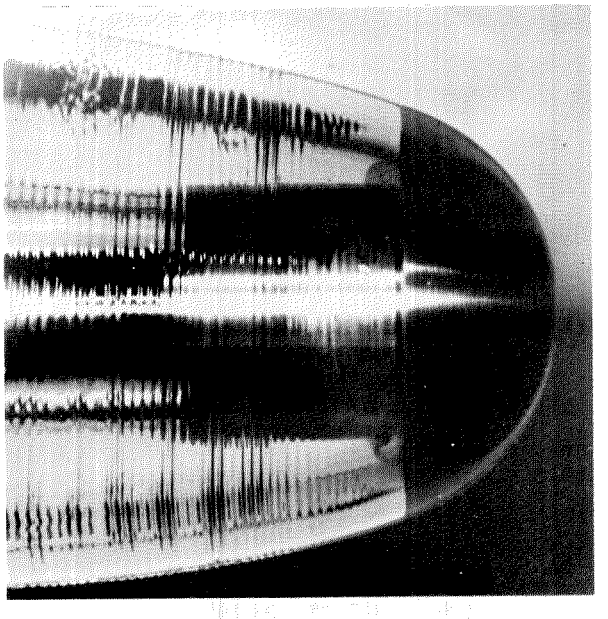

Plate 6. Cut-away Sphere.
Ventilated. U_T = 12 fps.

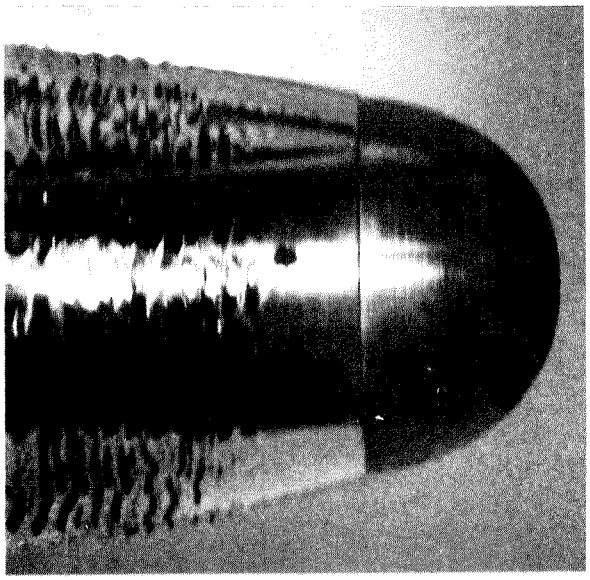

Plate 7. $1\frac{1}{8}$ in. Sphere. U_T=15 fps.
Ventilated cavity.

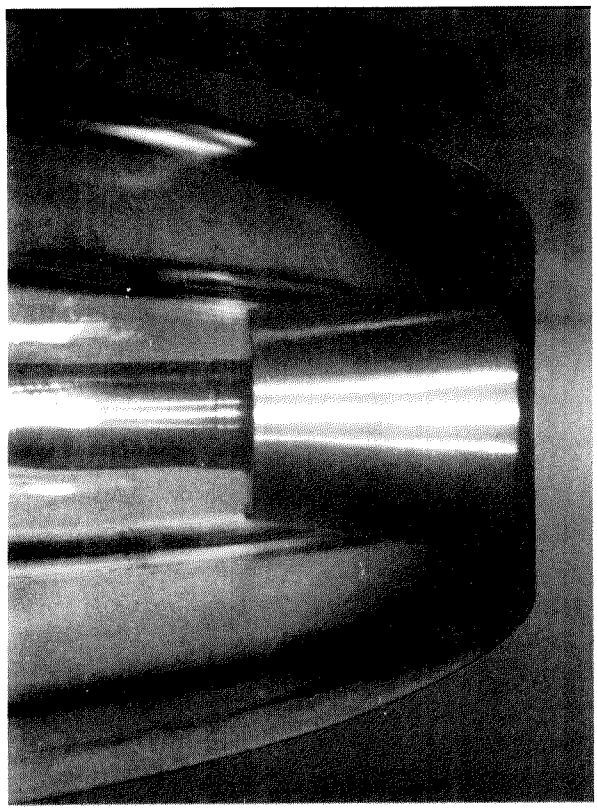

Plate 8. Disc. U_T=35 fps.
Ventilated cavity.

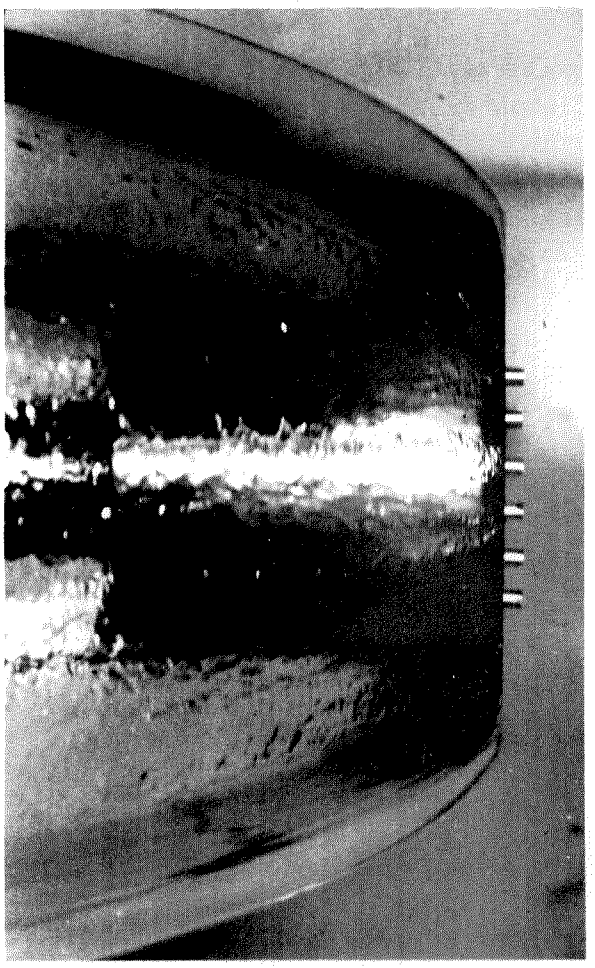

Plate 9. Disc with row of pegs on face. U_T=30 fps.
Ventilated cavity.

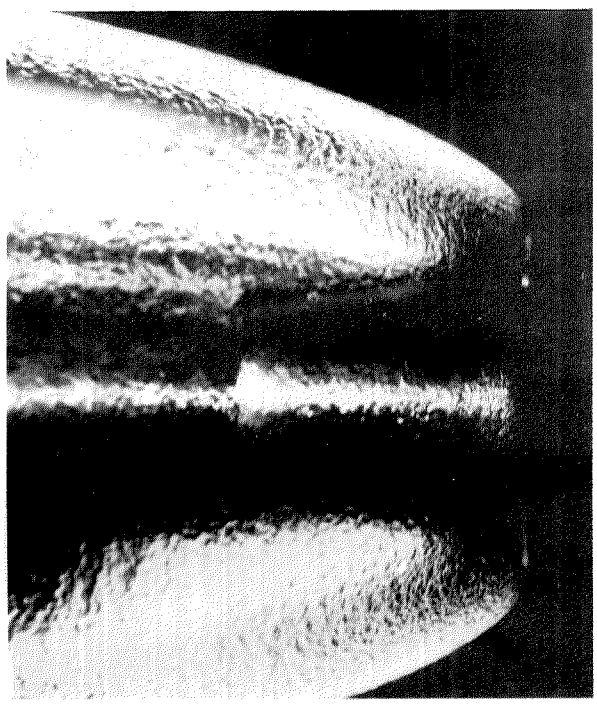

Plate 10. Disc with ring on face. U_T=30 fps.
Ventilated cavity.

Distribution

Froude Committee	(20)
Ship Model Laboratories	(30)
Shipbuilders and Shipowners	(35)
Universities	(25)
N.P.L. Staff	(30)
Ship Office	(60)